Factors affecting the formation of Insulin Amyloid Spherulites

Michael I. Smith[a,1], Vito Foderà[b, 1, *], James S. Sharp[a,c, *], Clive J. Roberts[c,d] and Athene M. Donald[b]

[a]School of Physics and Astronomy, The University of Nottingham, Nottingham, NG7 2RD, United Kingdom.

[b]Sector of Biological and Soft Systems, Department of Physics, Cavendish Laboratory, University of Cambridge, JJ Thomson Avenue, Cambridge CB3 0HE, United Kingdom.

[c]Nottingham Nanotechnology and Nanoscience Centre, The University of Nottingham, Nottingham, NG7 2RD, United Kingdom.

[d]Laboratory of Biophysics and Surface Analysis, School of Pharmacy, The University of Nottingham, Nottingham, NG7 2RD, United Kingdom.

[1]V.F. and M.I.S. equally contributed to the work and should be considered as first co-authors.

***Corresponding Authors**:

Vito Fodera', Sector of Biological and Soft Systems, Department of Physics, Cavendish Laboratory, University of Cambridge, JJ Thomson Avenue, Cambridge CB3 0HE, United Kingdom E-mail: vf234@cam.ac.uk Phone +44 0122 3337290. Fax +44 (0)1223 337000.

James S. Sharp, School of Physics and Astronomy, The University of Nottingham, Nottingham, NG7 2RD, United Kingdom. E-mail: James.Sharp@nottingham.ac.uk Phone +44 0115 95 15142.

Abstract

Thermally induced amyloid aggregation of bovine insulin can produce a number of distinct aggregate morphologies. In this work amyloid spherulites were analysed using cross polarized optical microscopy and light scattering. A new semi-quantitative methodology to estimate the balance of spherulites and free fibrils is reported and, from this analysis, the effects of pH, temperature, salt, and protein concentration on spherulite formation were quantitatively determined for the first time. The number and size of spherulites measured with polarized light microscopy were related to changes in the colloidal stability of the solution and fibril nucleation times (measured by static light scattering). Importantly, changes in pH between 1.75 and 2 were found to result in a dramatic decrease in the spherulite radii, which were related to differences in the conformational stability of the protein. Moreover, estimates of the final spherulite volume fraction clearly indicate that amyloid spherulite formation is the dominant pathway for insulin aggregation in HCl solutions at low pH and protein concentrations below ~5mgml^{-1}, with the balance shifting towards fibrils as the concentration increases.

Keywords: Amyloid Spherulites, Amyloid Fibrils, Nucleation, Cross polarized optical microscopy, TEM, Light Scattering.

1. Introduction

Developing a comprehensive understanding of the mechanisms by which protein in the native state may misfold and aggregate represents one of the major challenges in current biomedical research. Moreover, clarifying basic aspects of protein stability/aggregation is of considerable importance to the pharmaceutical and food industries [1, 2]. Fundamental understanding in this area also helps to elucidate the mechanisms governing the origin of amyloid fibrils and their relevance to diseases like Alzheimer's, Parkinson's and Type-II Diabetes [3-5]. Amyloid fibrils have been connected with the onset of such diseases, although their role is still a matter of debate, with some studies suggesting prefibrillar species may be the cytotoxic species [6-9]. These amyloid fibrils consist of linear chains of misfolded protein containing large amounts of intermolecular beta-sheet. Under appropriate experimental conditions (typically low pH and elevated temperature), the formation of such structures can also be induced *in vitro*. This is true for a large number of proteins, some of which are not related to disease, suggesting that amyloid fibril formation is a generic property of proteins.

Rationalizing the multistep process leading to fibril formation is challenging due to a number of contributing interactions, which occur on different time and length scales [10-12]. After a partial destabilization of the native structure, the formation of an assumed high energy species (*nucleus*) is believed to represent the first stage of aggregation. This is followed by subsequent elongation through addition of either monomeric or multimeric non-native protein, leading to the formation of protofibrils and then fibrils [13]. Moreover, fibrils can conserve their basic structural arrangement of cross β-sheet [14, 15], yet may experience different packing into three dimensional superstructures, such as amyloid spherulites [16].

Insulin is a model protein with a largely α-helical structure and it is commonly used for *in vitro* studies of fibril formation [17, 18]. Under specific conditions, i.e. low pH and high temperature, the protein rapidly converts into amyloid fibrils [17]. The use of such acidic conditions is common in

the pharmaceutical preparation of recombinant human insulin [18], where the production of fibrils, spherulites or nuclei would compromise the quality of the product. Specifically for insulin, several different insulin fibrillar morphologies have been reported in the past, ranging from straight and elongated fibrils, through spherulites [16], branched and twisted fibrils to superstructures of fibrils [19, 20].

Amyloid spherulites form during *in vitro* aggregation, not only for insulin [16] but also for other globular proteins such as HSA [21] and β-lactoglobulin [22, 23]. They have also been observed *in vivo* for the protein $A\beta_{42}$ [24]. Amyloid spherulites are readily identified when imaged using polarized light microscopy, by the characteristic Maltese cross pattern seen under crossed polarizers [16]. They consist of a central part, likely formed by non-specific protein aggregation, surrounded by radially oriented amyloid fibrils [25]. Under strongly acidic conditions, where the solution pH is far from the isoelectric point of the protein, these spherical aggregates can coexist with free fibrils [26]. In a previous study, it was proposed that a spherulite precursor is formed *via* non-specific aggregation [26]. In this paper we will use the term "precursor" to describe the initial non-specific aggregation which forms the subsequent centre of spherulites. Once this precursor is formed, radial fibril growth is observed [25] supporting the idea that the spherulites grow by sequential addition of protein molecules or oligomers rather than from preformed fibrils.

Here, a combination of polarized light optical microscopy and static light scattering was used to investigate the effect of temperature, salt, pH and protein concentration on the propensity of bovine insulin to form amyloid spherulites and free fibrils. Previous studies from our group reported the effect of temperature, salt and protein concentration on spherulite growth using time-lapse microscopy analysis on a statistical ensemble of ~20 spherulites [23, 27]. These studies allowed the rationalization of the kinetics of spherulite growth in terms of a population-based polymerization model [23], enabling the quantification of growth rate and appearance time for each spherulite [23, 27]. However, such studies based on kinetics analysis do not provide information on the different propensity of the protein to forming spherulites under different environmental conditions. As a

consequence, a number of questions remain unanswered: in particular, what are the effects of temperature, salt concentration, pH and protein concentration on the probability of spherulite formation (i.e. final number of spherulites)? Which of these parameters affect the balance between free fibrils and amyloid spherulites? To answer these questions, a truly statistical and direct investigation (as opposed to measurements of isolated spherulites) would be required and, to the best of our knowledge, has not been attempted. We develop a semi-quantitative methodology that samples the distribution of spherulite sizes (an ensemble of ~4000 - 15000 spherulites) and enables us to make not only measurements of isolated spherulite radii, but also quantitative estimates of the number and volume fraction of spherulites present under different environmental conditions. Using this approach and varying the above mentioned parameters, changes in the final size and number of spherulites were related to the colloidal and conformational stability of the protein molecules. Importantly the analysis reported here shows that there is an unexpected and non-trivial dependence of spherulite radii on pH between 1.75 and 2. Moreover, analysis of the volume fraction of protein also shows that the occurrence of spherulites is not a minor contribution, but actually represents the dominant pathway for insulin aggregation at low pH, with the balance shifting towards free fibrils at high protein concentrations (>5mgml-1).

2. Materials and Methods

2.1 Sample preparation

NaCl solution (50mM) was prepared and filtered with a 0.2µm syringe filter (Sartorius, MS16534), to remove any salt crystals. This was combined with HCl solutions in a 1:1 ratio to give a final stock solution of pH 2, 25mM NaCl. Bovine Insulin (BPI) was obtained as a lyophilised powder from Sigma Aldrich (I5500) and dissolved at the desired protein concentration in the stock solution. Once all the protein had dissolved, the pH of the solution was adjusted to pH 1.75 using concentrated HCl. The solution was then filtered using a 300kDa (~20nm) [28] Vivaspin 2 filter

(Sartorius). A small quantity of (~100nm) aggregates were found to form when the filters were centrifuged so the samples were simply allowed to filter under gravity. The 100 nm aggregates did not form when the samples were filtered in this way. Dynamic light scattering of the filtered solutions confirmed that this resulted in a monomodal size distribution of protein structures with a mean diameter of 3.5 ± 1.0 nm (consistent with the hydrodynamic diameter of the insulin monomer) [29]. UV-vis absorbance measurements at 276 nm also confirmed that the concentration of protein before and after was not appreciably altered by the filtration step. Solutions were also prepared with different concentrations of salt and protein, as specified in the text below. In each case, the addition of the protein powder was found to change the pH of the solution. Depending upon the final desired pH, two stock solutions of pH 2 and pH 3 were used to dissolve the protein. The solutions were then adjusted to the required pH using concentrated HCl with a measured accuracy of pH ± 0.01. Importantly, H^+ titration curve for insulin was shown to be not affected by the history of pH adjustment.

2.2 Optical microscopy measurements of amyloid spherulites.

Vials of protein solution were incubated at 60-90^{o}C for 18 hours in a heated metal block. Following heating, the vials were gently turned end over end to ensure a uniform distribution of protein aggregates. Small aliquots of aggregated protein solutions (7.5μL) were carefully drawn from the vials and deposited onto a glass microscope slide. A circular glass coverslip was then placed on top of the droplet causing the solution to spread out over the entire area of the coverslip. Five images were then taken at different locations on the sample using a x10 microscope objective. The images were collected using crossed polarisers which enabled spherulites to be easily distinguished from the background by the characteristic Maltese cross (see figure 1) [16]. This was repeated for 20 aliquots of each vial measured. Since many amyloid spherulites were found to cluster, it was not possible to count the large number and radius of spherulites automatically. A semi-quantitative estimate of the number of spherulites was therefore obtained in the following way. Image pro plus

4.0 software (Media Cybernetics) was used to measure the total area (A_{Sph}) covered by spherulites (clustered and isolated) in all of the one hundred images (the spherulites were distinguished by their colour, relative to the background). In order to ensure that the Maltese cross of the spherulites was included in this area, a strongly scattering foam was placed under the glass slide. This resulted in the Maltese cross of the spherulites appearing a slightly different colour to the image background and enabled the cross to be distinguished by the software. The radius (r_i) of 500 isolated spherulites was also measured manually from representative images and the mean area of an individual spherulite was calculated for each set of conditions. The total number of spherulites (N_{Sph}) was then obtained by dividing the total area of spherulites (A_{Sph}) by the mean area obtained from isolated spherulites (A_{mean}) using the following equation.

$$N_{Spherulite} \approx \frac{A_{Sph}}{A_{mean}} = \frac{500 A_{Sph}}{\sum_{i=1}^{500} \pi r_i^2} \quad (1)$$

If the density of native protein molecules does not change when incorporated into a spherulite then the volume fraction is:

$$\varphi_{Spherulite} \sim \frac{V_{Sph}}{V_{Protein}} = \frac{N_{Sph}\langle R_{Sph}^3 \rangle}{N_{Protein}\langle R_{Protein}^3 \rangle} \quad (2)$$

where R_{Sph} is the mean spherulite radius, V_{Sph} *and* $V_{protein}$ are the volume of protein in spherulites and the total volume of protein, $N_{Protein}$ is the number of protein molecules in solution and $R_{Protein}$ is the radius of a single protein molecule.

The value chosen for the protein radius critically affects the values obtained for the volume fraction. An appropriate range of values for the radius of an insulin molecule is between the hydrodynamic radius (~2 nm) [30] and the radius of gyration (1.16 nm) [17]. A homogeneous sphere with a radius of gyration R_g has a radius $R=R_g(5/3)^{0.5}$ [29]. The radius of a protein chain in the absence of a hydrodynamic layer will therefore equal 1.50nm in our calculations.

2.3 Static light scattering measurements.

Samples were placed in a heated block and illuminated with laser light (λ = 632 nm). The intensity of scattered light collected at 90 degrees to the incident beam, was measured with a photomultiplier tube during incubation of the solutions. The time evolution of the intensity was obtained for samples at different temperature (60-90 ^{o}C), pH (1- 2.5) and protein concentration (1-10 mgml^{-1}) and the nucleation times were determined.

2.4 TEM measurements of amyloid fibrils.

A population of free fibrils was observed to coexist with amyloid spherulites. The fibrils were imaged with transmission electron microscopy according to a standard protocol: Copper 400 mesh grids (Agar Scientific, Stansted, U.K.) were coated with Formvar and carbon film. Insulin solutions containing amyloid fibrils were diluted 50-fold in eppendorf tubes, and 3.5-µl aliquots were placed on the grids. After 60 s, 10 µl of distilled water were added and then excess water was removed. Then, 10 µl of 2% uranyl acetate (Agar Scientific) was placed on the grid and left for 30 s. Finally, two 10 µl drops of distilled water were added and again excess water removed. The grid was then left to dry. Images were collected using transmission electron microscopy (Technai 20, FEI) operating at an acceleration voltage of 120 kV and magnifications typically around x26,000. Statistical analysis of the fibril length was performed by analyzing up to ~ 40 representative images for each sample. The fibril lengths were then manually measured using an open source program (Image J software).

3 Results and Discussion

3.1 Effect of temperature and salt on spherulite formation.

The effect of temperature on spherulite formation was investigated in the range 60-90˚C using insulin solutions containing 4mgml^{-1} BPI, 25mM NaCl, pH 1.75. The spherulite and fibril content of samples were also explored systematically, using a range of NaCl concentrations 0-100 mM

(4mgml^{-1} BPI, at pH 1.75, and 60˚C). In this range of conditions (low pH and high temperature) spherulites and free fibrils were observed to coexist, as has previously been documented [26].

Typical images obtained by polarised light optical microscopy at 60 and 90˚C (25mM NaCl) are shown in figure 1a and 1b, respectively. Clear, qualitative differences can be seen in both the size and number of spherulites observed in each type of sample. At 60˚C small numbers of large spherulites were observed, (figure 1a) while at 90˚C, larger numbers of smaller spherulites were observed (figure 1b). This is confirmed by the quantitative analysis (see "Material and Methods" section) of the number (○) and radius (□) of spherulites at different temperatures shown in figure 1c.

The nucleation times associated with protein aggregation were measured using static light scattering. The measured intensity showed three distinct phases: a lag phase (see inset in figure 2a), a main growth phase and a phase with saturated intensity (figure 2a, main panel). The nucleation times (defined as the intersection of lines fitted to the lag and growth portions of the curve) show a clear temperature dependence, with the nucleation times decreasing with increasing temperature (figure 2b, inset). In the main panel of figure 2b, the radius (□) has been plotted as a function of the final number of spherulites for samples at 60, 70, 80 and 90˚C. The radius is found to decrease as the number of spherulites increases.

A qualitatively similar dependence of the radii and number of spherulites on salt concentration is also observed (figure 3). The average spherulite radius ranged from ~75µm at 0mM to ~5µm at 100mM NaCl. At 0 mM NaCl the central part of the spherulite (which was non-birefringent) was observed to occupy a larger fraction of the total volume of the spherulite than at higher salt concentrations [26]. In the absence of electrolyte the spherulites were isolated, but as the salt concentration was increased, dramatic clustering of small spherulites was observed (see insets figure 3). The clustering of spherulites at high salt concentrations (≥50mM NaCl) was so pronounced that quantitative analysis of the number of spherulites was not possible. However,

simple examination of the images obtained clearly showed that the numbers increased significantly with salt concentration.

Measurements of the lengths of free fibrils obtained from solutions with 0 or 100mM NaCl, were obtained by TEM analysis (see figure 4 and Material and Methods section for details). In the absence of salt (white columns), a wide distribution of lengths occurs with fibrils of up to ~ 20 μm (image on the right in figure 4) and a mean value of ~ 4 μm. However, in the presence of 100mM NaCl (black columns), this decreases to ~700 nm.

A single amyloid fibril grows via *nucleus* formation and subsequent elongation [3]. Spherulite growth is believed to occur with an initial formation (*via* nonspecific aggregation) of a precursor species from which multiple fibrils nucleate and grow radially [26]. The structure and composition of the precursor associated with spherulite formation is still unknown. However, it is expected that the final number of spherulites will be equal to the number of spherulite precursors formed in solution.

The data for size and number of spherulites presented in figures 1 and 2 can be described intuitively in terms of three key factors: i) colloidal stability, ii) conformational stability, and iii) the amount of available protein which is able to participate in spherulite formation. Increases in temperature or salt concentration both have a destabilizing effect by reducing both colloidal and conformational stability and increasing the rates of aggregation. Changing the salt concentration and temperature will affect two key parameters: namely the number of precursors present in solution prior to fibril growth, and the nucleation time at which the growth of fibrils begins. Increasing the temperature is expected to increase the number of spherulite precursors as shown in figure 1c (○). It is not known how the precursor arises. It could be a nucleation dependent process or a gradual coalescence and coarsening of smaller aggregates. Interestingly, light scattering measurements show a steadily increasing intensity in solution in the early stages of the process (see inset in figure 2a), which is in agreement with previous studies [19, 31]. Particles of a larger size scatter light more strongly, suggesting that some form of aggregation is gradually occurring well

before fibril nucleation. One expects that decreases in conformational and colloidal stability would increase the rates of precursor formation. However, such factors will also affect the rate of fibril nucleation at the spherulite precursor surface. The exact number of spherulite precursors will therefore depend on the relative rates of precursor formation and the fibril nucleation time. Once nucleation occurs on the surface of a spherulite precursor the number of spherulites is expected to remain approximately constant with fibril growth (either spherulites or free fibrils) expected to be the dominant process.

The volume fraction of insulin which forms spherulites was calculated, assuming that all insulin molecules under these conditions are converted into amyloid aggregates [32, 33]. This is a useful way of assessing the relative abundance of spherulite and fibrillar aggregates and can only be performed as a result of the statistically significant sample measured for each set of conditions. These calculations suggest that the majority of molecules are incorporated into spherulites (~80%), with a smaller fraction available to form free fibrils. This balance is apparently unaffected over the range of temperatures studied here (data not shown).

Surfaces have been shown to enhance the rate of fibril nucleation over that in bulk solution [20, 33-35]. Heterogeneous nucleation of fibrils would be expected to be catalysed by the precursor surface. The growth of fibrils around a spherulite precursor would therefore be favoured over that of free fibrils. This would explain why the balance of morphologies is dominated by amyloid spherulites at 4 mg ml^{-1}. The occurrence of free fibrils was verified using TEM (figure 4) for samples at 60˚C with 0mM and 100mM NaCl, and were found to be significantly shorter than the fibrils incorporated into spherulites. Fibril and spherulite growth under these conditions has been shown to be reaction rate limited [25]. This means that growth is not limited by diffusion of new molecules, but the rearrangement time associated with forming the correct protein conformations required for attachment to a growing fibril. It seems unlikely therefore that the local environment of a growing fibril tip (free fibril or in a spherulite) affects the growth rate. If fibrils at the spherulite precursor surface nucleate at earlier times, and grow at the same rate as free fibrils, then one would

expect fibrils incorporated in spherulite to be longer. The shorter measured lengths of free fibrils therefore support the idea that spherulite precursors catalyse fibril growth and act like nucleating agents.

The constant volume fraction also suggests a simple explanation for the data in figures 1 and 2. At low pH and high temperature, the addition of protein molecules to the end of a growing fibril (either free or in a spherulite) would be expected to continue so long as free protein remains available in solution. Since in these experiments samples were incubated until no further changes occurred (spherulites and fibrils being the only detectable aggregate species) [16, 25, 26 32, 35-38], it seems reasonable to assume that all protein is eventually incorporated into a free fibril or a growing spherulite. In this scenario, the average size of spherulites would then be determined by the finite amount of protein in the system and the number of precursors from which fibrils can grow. If sizes are governed by the limited concentration of protein the volume of protein in spherulites should be a conserved quantity. The volume is proportional to NR^3 (where N is the number of spherulites/precursors and R is the mean final spherulite radius, both of them temperature dependent) so for a given number of spherulites N under specific conditions:

$$R(N) = (N_{T=60}/N)^{1/3} R_{T=60} \qquad (3)$$

where $N_{T=60}$ and $R_{T=60}$ are the number and mean radius measured at 60˚C. The solid line in figure 2b represents the prediction of equation 3 and shows good agreement with the experimental data (open squares). This provides convincing evidence of the basic picture proposed.

3.2 pH dependent study.

Figure 5 shows how spherulite radii vary with the pH of the solution. We find the same trend for all protein concentrations. At low pH (1-1.75) the radius increases systematically with pH. It is worth noting that differences in aggregation must largely depend on either differences in colloidal stability or sticking probability due, for instance, to conformational changes in the protein structure.

Colloidal stability is determined by the DLVO potential surrounding each protein. This is affected by both charge and electrolyte screening effects [39]. The electrolyte concentration of NaCl in the pH dependent experiments was kept constant. However, the electrolyte concentration is determined not just by NaCl concentration but also by free H^+ and Cl^- ions in solution [40]. A lowering of the pH will therefore increase the screening of the protein in the same manner achieved by adding salt. Based upon the arguments presented above and on the results discussed in section 3.1, decreasing the colloidal stability decreases the radius of spherulites. This is in agreement with what is observed in the region pH 1-1.75 (Figure 5).

At pH 1.75 – 2 an abrupt change is observed in the size of the final spherulites which is unlikely to be purely due to factors affecting colloidal stability. Haas and co-workers [41] examine the conformational flexibility of bovine insulin as a function of pH. In simulations of the conformational space sampled by the protein chain they found a significant difference in behaviour in the regions pH 1-2 and 2-5: the C terminal of the B chain on the insulin molecule can sample a much wider conformational space at higher pH resulting in a significant difference in the entropic contribution to the free energy barrier. The B-chain's C-Terminal is known to play an important role in insulin fibrillation. Brange and co-workers suggest that the B-chain's C terminus must be displaced in order to expose key hydrophobic residues involved in fibril formation [42]. Moreover, insulin degradation at the Asn21 residue can occur under these highly acidic conditions providing an alternative possible explanation of the observed effects [43]. However it should be noted that the crystal structure at pH 2 shows no evidence of degradation [44]. A higher conformational flexibility of this terminal would therefore lead to a higher probability of the molecule losing its native structure under conditions conducive to aggregation. For this reason, the pH dependent flexibility of insulin would be expected to sharply influence the aggregation of all insulin amyloid aggregates.

If the free energy barrier to amyloid fibril formation was reduced by a difference in conformational flexibility, one would expect a reduction in the fibril nucleation time at a pH ~ 2. In figure 6, light scattering measurements show that this is indeed observed. A reduction in the

nucleation time, from our previous results would lead us to expect a reduction in the size of observed spherulites due to the presence of larger numbers of precursors in solution. The size dependence of spherulites in this region is therefore determined by a complex interplay of both colloidal and conformational stability. Changes in pH alter the DLVO potential and may have a specific effect between pH 1.75-2 on the ability of insulin to sample conformations that are conducive to amyloid fibril formation. It is important to note that these two effects together would alter both the speed of precursor formation and fibril nucleation times. This combination of factors results in a non-trivial spherulite size dependence at the higher pH values.

3.3 Protein Concentration.

The effect of initial protein concentration, in the range 1-10 $mgml^{-1}$, on spherulite formation was also systematically investigated (pH 1.75, 25mM NaCl, T=60˚C). The radius of spherulites was found to increase approximately linearly with increasing protein concentration (see top right inset in figure 7, ○). The number of spherulites displays an unexpected concentration dependence (see bottom left inset in figure 7). The number of spherulites increases with concentration up to a maximum at $4mgml^{-1}$ which would be expected since the presence of more protein molecules should increase the probability of any two molecules interacting and so will produce more precursors. As the concentration continues to be increased, however, the numbers of observed spherulites decrease. An instructive quantity is the volume fraction of protein incorporated into spherulites (see equation 2) as it isolates changes due to the presence of more molecules from more fundamental differences in spherulite formation (see figure 7 main panel). At concentrations below ~ $5mgml^{-1}$ figure 7 shows that an increase in concentration has little effect upon the final fraction of protein incorporated into amyloid spherulites. In this regime figure 7 shows that the majority of the protein present in solution forms part of a spherulite. We note as above that the precise magnitude of the volume fraction is dependent upon the value chosen for the protein radius, although the observed trend is independent of such details. Inspection of samples of different protein

concentrations after incubation (pH 1.75, 25mM NaCl, T=60˚C) showed that protein concentrations grater than ~5mgml^{-1} caused the samples to form a gel. In contrast, at protein concentrations less that 5mgml^{-1} the samples contained weakly associated agglomerates that were easily dispersed upon gentle shaking of the vial.

Extension of the arguments (relating spherulite numbers to final radius) presented above to the possible effects of protein concentration on the final radii of spherulites enables us to develop a simple scaling to calculate spherulite radius. By scaling to a "standard" condition of T=60˚C, 4mgml^{-1}, pH 1.75, 25mM NaCl and assuming a complete conversion into spherulites and fibrils, we can write a general expression for the radius as a function of concentration and the number as.

$$R(C,N) = \left(\frac{C}{N}\frac{N_{T=60}}{C_{T=60}}\right)^{1/3} R_{T=60} \qquad (4)$$

The top right inset in figure 7 shows that below ~5mgml^{-1} the size experimental data (○) are well described by equation 4 (Δ) indicating that below this concentration it is indeed the finite amount of protein that controls the final spherulite radius. Above 5mgml^{-1}, although spherulite radii continue to increase, the number (see bottom left inset in figure 7) and consequently the volume fraction of spherulites decreases significantly with increasing protein concentration. The precise reason for this reduction is unclear but fits well with our previous observations performed under similar conditions and high concentrations [34, 45]. Importantly, this suggests that the shift in the balance between fibrils and spherulites is related to a change in the number of spherulite precursors that are present in solution. This is influenced strongly by protein concentration.

At protein concentrations greater than 5mgml^{-1}, the volume fraction of spherulites present in solution decreases with a corresponding rise in free fibrils. Entanglement of a sufficient numbers of polymers may lead to gelation. In a solution of large numbers of free fibrils (> 5mgml^{-1} figure 7), entanglement of the fibrils would be expected to result in the formation of a percolating network and hence gel formation. Conversely, at lower protein concentrations the predominance of spherulites results in large amounts of protein being localised in small volumes of the solution with

less possibility of entanglement. The onset of gelation observed is therefore likely to be a consequence of the shift in the balance between spherulites and fibrils with concentration.

4 Conclusions

In this work a comprehensive investigation of amyloid spherulite formation in bovine insulin samples as a function of pH, salt, protein concentration and temperature has been presented. A new semi-quantitative methodology was developed to provide a statistically significant analysis of the final abundance of amyloid aggregates and the balance of aggregate morphologies. Such approach allowed us to extend the range of parameters studied (i.e. the number and volume fraction of spherulites) in comparison with earlier studies mainly focused on the growth rates and appearance times of isolated number of spherulites [23, 27]. Moreover, the effect of the pH on the spherulite radius is here reported for the first time.

Analysis of the experimental data as a function of pH, temperature and salt concentration, was interpreted in terms of the colloidal and conformational stability of the protein molecules in a solution coupled with the finite quantity of protein available. These factors affect both the number and the size of the spherulites without changing the balance between free fibrils and spherulites. Two distinct pH regions were identified with large changes in spherulite radius occurring between pH 1.75 and 2. Importantly, protein concentration was shown to affect the balance between free fibrils and spherulites, with the volume fraction of free fibrils increasing with concentration above 5 $mgml^{-1}$. At low pH, elevated temperature (60-90˚C), 25mM NaCl and for protein concentrations below ~ $5mgml^{-1}$, amyloid spherulites were observed to be the dominant pathway for bovine insulin.

Acknowledgments Funding from the EPSRC (EP/H004939/1) is gratefully acknowledged.

References

[1] E.Y. Chi, S. Krishnan, T.W. Randolph, J.F. Carpenter, Pharm. Res. 20 (2003) 1325.

[2] D.M. Mulvihill, J.E Kinsella, Food Technol 41 (1987) 102.

[3]. F. Chiti, C.M. Dobson, Annual Review Biochemistry 75 (2006) 333.

[4] F. Chiti, P.Webster, N. Taddei, A. Clark, M. Stefani, G. Ramponi, C.M. Dobson Proc. Natl. Acad. Sci. 96 (1999) 3590.

[5] M. Vendruscolo, J. Zurdo, C.E. MacPhee, C.M. Dobson, Phil. Trans. R. Soc. Lond. A 361 (2003) 1205.

[6] R. Kayed, E. Head, J.L. Thompson, T.M. McIntire, S.C. Milton, C.W. Cotman, C.G. Glabe, Science 300 (2006) 486.

[7] B.M. Austen, K.E. Paleologou, S.A. Ali, M.M. Qureshi, D. Allsop, O.M.A. El-Agnaf, Biochemistry 47 (2008)1984.

[8] Y. Yoshiike, T. Agaki, A. Takashima, Biochemistry 46 (2007) 9805.

[9] A.D. Williams, M. Sega, M. Chen, I. Kheterpal, M. Geva, V. Berthelier, D.T. Kaleta, K.D. Cook, R. Wetzel, Proc. Natl. Acad. Sci. 102 (2005) 7115.

[10] V.N. Uversky, A.L. Fink, Biochim. Biophys. Acta 1698 (2004) 131.

[11] V. Militello, C. Casarino, A. Emanuele, A. Giostra, F. Pullara, M. Leone, Biophys. Chem. 107 (2004) 175.

[12] V. Vetri, C. Canale, A. Relini, F. Librizzi, V. Militello, A. Gliozzi, M. Leone, Biophys. Chem. 125 (2007)184.

[13] F. Ferrone, Methods Enzymol. 309 (1999) 256.

[14] M. Fändrich, J. Meinhardt, N.Grigorieff, Prion 3 (2009) 89.

[15] J. Meinhardt, C. Sachse, P. Hortschansky, N. Grigorieff, M. Fändrich J Mol Biol. 386(2009) 869.

[16] M.R. Krebs, C.E. Macphee, A.F. Miller, I.E. Dunlop, C.M. Dobson, A.M. Donald, *Proc Natl Acad Sci* 101 (2004) 14420.

[17] L. Nielsen, R. Khurana, A. Coats, S. Frokjaer, J. Brange, S. Vyas, V. N. Uversky, A. L. Fink, Biochemistry 40 (2001) 6036.

[18] A. Ahmad, V.N. Uversky, D. Hong, A.L. Fink, J Biol Chem. 280 (2005) 42669.

[19] M. Manno, E.F. Craparo, A. Podestà, D. Bulone, R. Carrotta, V. Martorana, G. Tiana, San P.L. Biagio, J. Mol. Biol. 366 (2007) 258.

[20] V. Foderà, M. van de Weert, B.Vestergaard, Soft Matter 6 (2010) 4413.

[21] J. Juárez, P. Taboada, S. Goy-López, A. Cambón, M.B. Madec, S.G. Yeates, V. Mosquera, J. Phys. Chem. B 113 (2009) 12391.

[22] S.G. Bolder, H. Hendrick, L.M. Sagis, E. van der Linden, J Agric Food Chem. 54 (2006) 4229.

[23] K.R.Domike, A.M.Donald, Biomacromolecules 8 (2007) 3930.

[24] C. Exley, E. House, J.F. Collingwood, M.R. Davidson, D. Cannon, A.M. Donald, J. Alzheimers Dis. 20 (2010) 1159.

[25] S.S. Rogers, M.R.H. Krebs, E.H.C. Bromley, E.van der Linden, A.M. Donald, Biophys. J. 90 (2006) 1043.

[26] M.R. Krebs, E.H. Bromley, S.S. Rogers, A.M. Donald, Biophys J. 88 (2005) 2013.

[27] K.R. Domike, A.M. Donald Int. J. Biol. Macromolecules 44 (2009) 301

[28] Y. Wyart, G. Georges, C. Deumie, C. Amra, P. J. Moulin, Journal of Membrane Science 315 (2008) 82.

[29] L. Hovgaard, H. Jacobs, N.A. Mazer, S.W. Kim International J. Pharmaceutics 132 (1996) 107.

[30] M. Lunn, A first course in mechanics Oxford Science Publications 1991.

[31] V. Foderà, S. Cataldo, F. Librizzi, B. Pignataro, P. Spiccia, M. Leone, J. Phys. Chem. B 113 (2009)10830.

[32] B. Vestergaard, M. Groenning, M. Roessle, J. S. Kastrup, M. van de Weert, J. M. Flink, S. Frokjaer, M. Gajhede, D. I. Svergun, PLoS Biol. 5 (2007) 1089.

[33] V. Foderà, F. Librizzi, M. Groenning, M. van de Weert, M. Leone, J. Phys. Chem B 112 (2008) 15174.

[34] M.I. Smith, J.S. Sharp, C.J. Roberts, Biophys. J. 93 (2007) 2143.

[35] V. Sluzky, J.A. Tamada, A.M. Klibanov, R. Langer, Proc. Nati. Acad. Sci. 88 (1991) 9377.

[36] R. Jansen, W. Dzwolak, R. Winter, Biophys J. 88 (2005) 1344.

[37] S. Grudzielanek, V. Smirnovas, R. Winter, J Mol Biol. 356 (2006) 497.

[38] V. Foderà, A.M. Donald, Eur. Phys. J. E Soft Matter 33 (2010) 273.

[39] J. Israelachvilli, Intermolecular and Surface Forces Academic Press 1985.

[40] B. Bekard, D.E. Dunstan, Biophysical J. 97 (2009) 2521.

[41] J. Haas, E. Vöhringer-Martinez, A. Bögeholdm, D. Matthesm, U. Hensenm, A. Pelahm, B. Abel, H.Grubmüller, Chembiochem. 10 (2009) 1816.

[42] J. Brange, L. Andersen, E.D. Laursen, G. Meyn, E. Ramussen, J. of Pharmaceutical Sciences 86 (1997) 517.

[43] J. Brange Stability of insulin: studies on the physical and chemical stability of insulin in pharmaceutical formulation, Kluwer Academic Publishers, 1994

[44] J.L. Whittingham, D.J. Scott, K. Chance, A. Wilson, J.Flich, J. Brange, G.G. Dodson Journal of Molecular Biology 318 (2002) 479.

[45] M.I. Smith, J.S. Sharp, C.J Roberts, Biophys J.95 (2008) 3400.

FIGURE 1

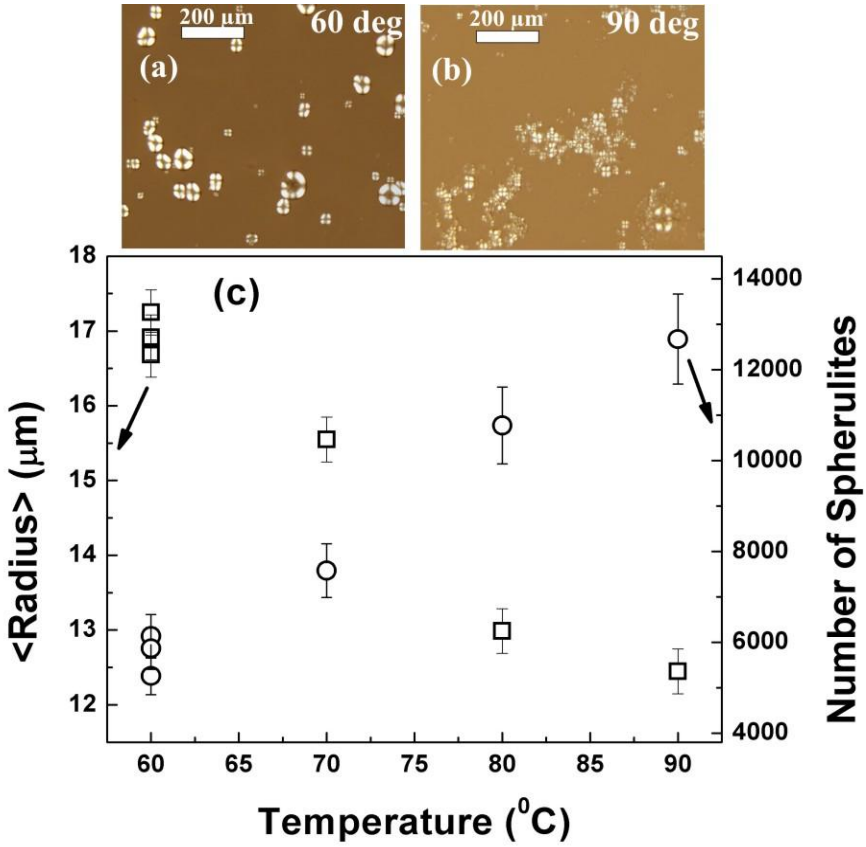

FIGURE 1 Temperature dependence of amyloid spherulite formation. Optical microscope images of spherulites at (a) 60˚C and (b) 90˚C viewed between crossed polarisers; (c) the mean radius (□) and estimated number (○) of Amyloid Spherulites in 25µL of solution grown at different temperatures (4mgml^{-1} BPI, 25mM NaCl, pH 1.75).

FIGURE 2

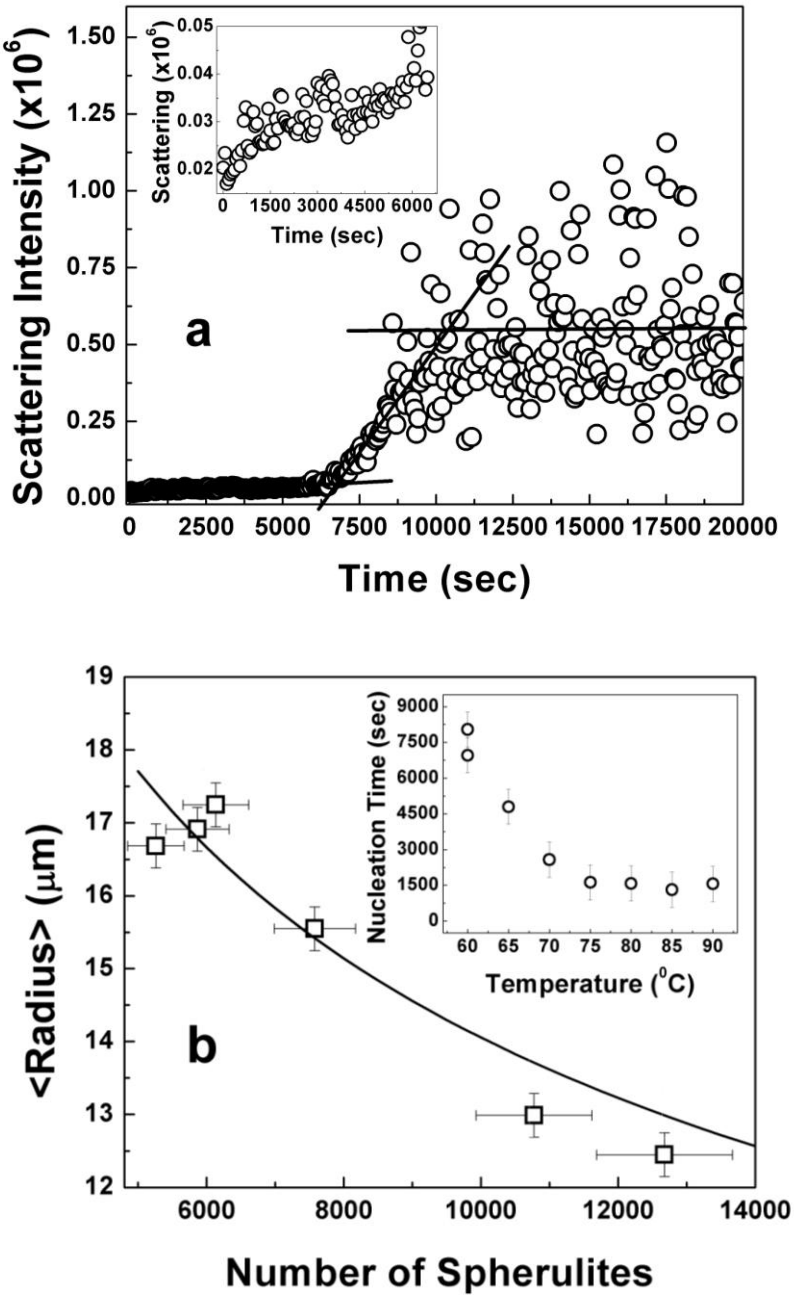

FIGURE 2 a) Main panel: example of static light scattering kinetics during the incubation of a sample of 4mgml^{-1} BPI pH 1.75 25 mM NaCl at 60 ˚C. Inset shows the increase of the signal in the early stages. Intersection of lines fitted to the lag and growth portions of the curve are used for the estimation of nucleation times. b) Controlling the size and number of spherulites. Main panel: mean spherulite radius as a function of the number of spherulites in 25 μL of solution (□). Inset: the

nucleation times measured at different temperatures. Samples were 4mgml^{-1} BPI, 25mM NaCl, pH 1.75. Solid line represents the relationship between spherulite radius and number of spherulites as predicted by equation 3 (see text).

FIGURE 3

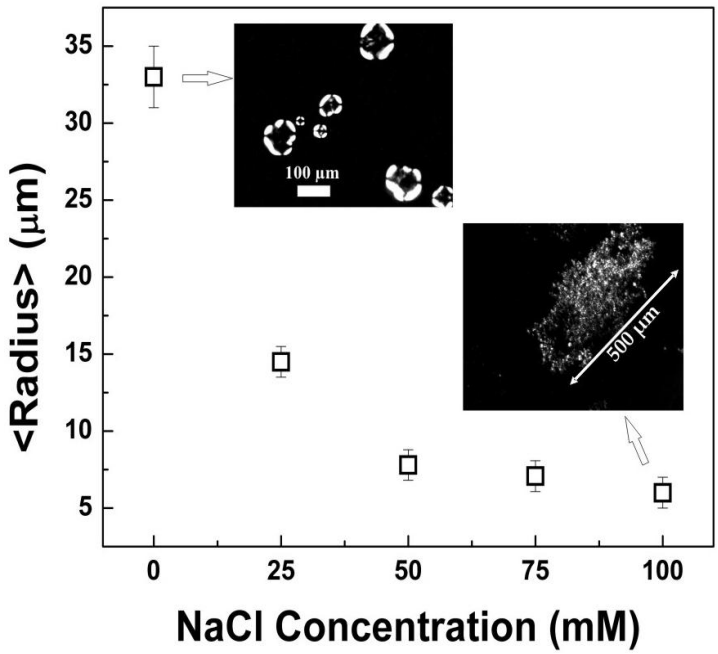

FIGURE 3 The mean radius of spherulites (4mgml^{-1} BPI, pH 1.75, T=60˚C) as a function of the salt concentration. Insets show typical images of spherulites at 0mM (left) and 100mM (right) viewed between crossed polarisers.

FIGURE 4

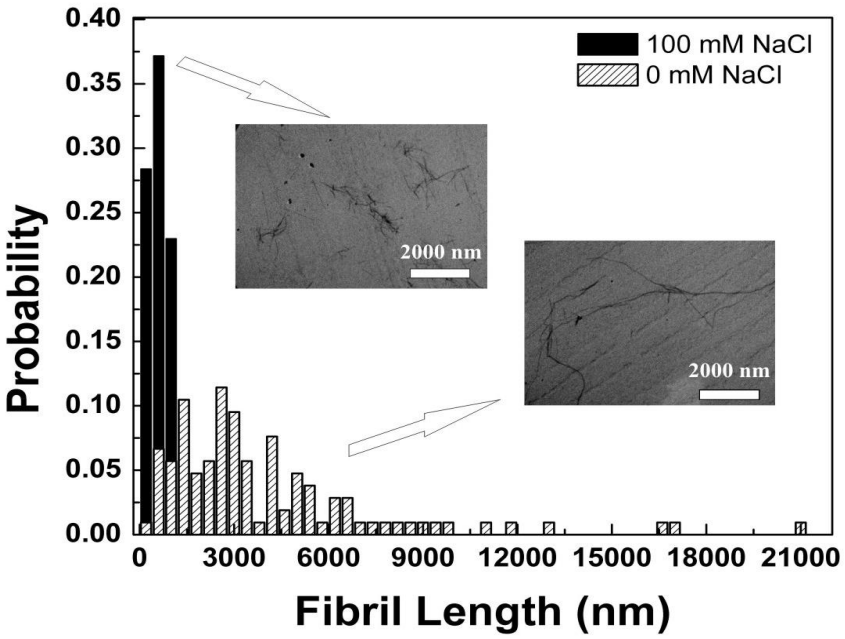

FIGURE 4 Fibril length distributions for 0 and 100mM NaCl concentration (4mgml^{-1}, T=60˚C, pH 1.75). The insets show typical images of fibrils under the two conditions. Increasing NaCl concentration results in a reduction in the length of fibrils. The lengths of 100 (0mM NaCl sample) and 160 (100 mM NaCl sample) fibrils were measured.

FIGURE 5

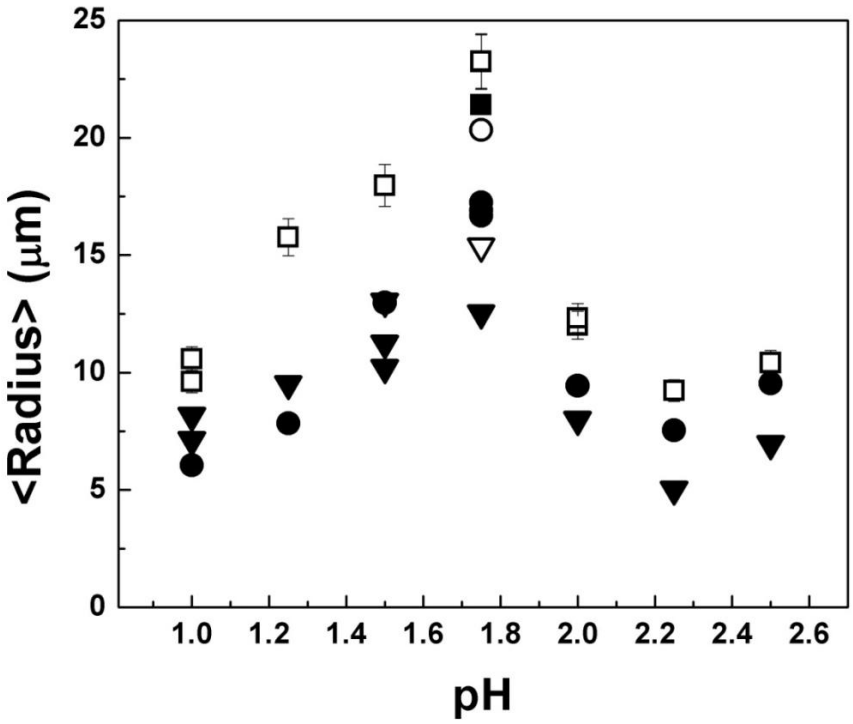

FIGURE 5 The mean radius of spherulites incubated at 60˚C (25mM NaCl) as a function of pH and at different BPI concentrations.. Concentrations of 10 (□), 8.5 (■), 7 (○) , 4 (●), 2.5 (▽) and 1 (▼) $mgml^{-1}$.

FIGURE 6

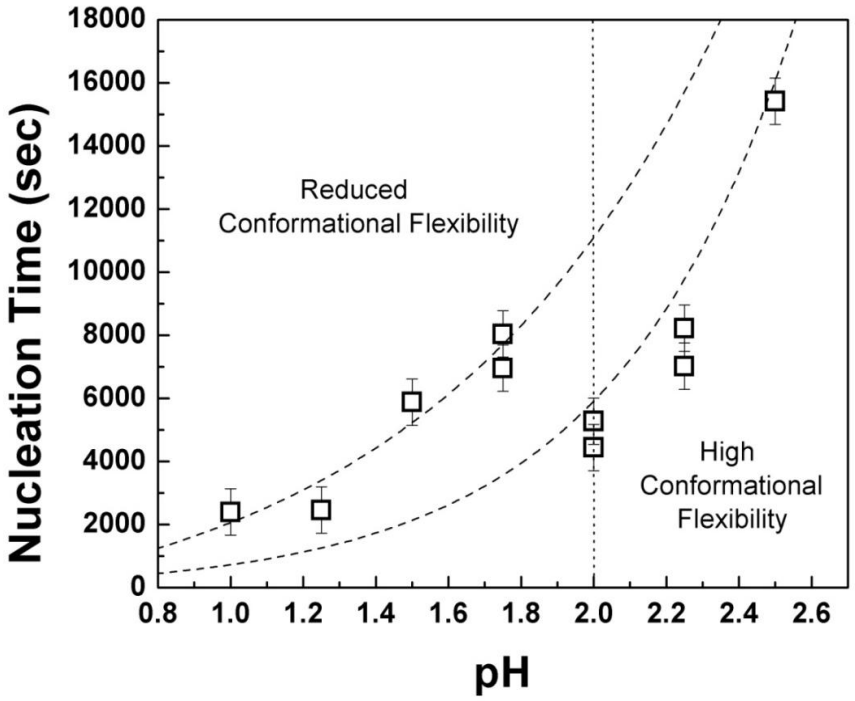

FIGURE 6 The influence of pH on fibril nucleation times (4mgml^{-1} BPI, 25mM NaCl, T=60˚C). Dashed lines are guides to the eyes.

FIGURE 7

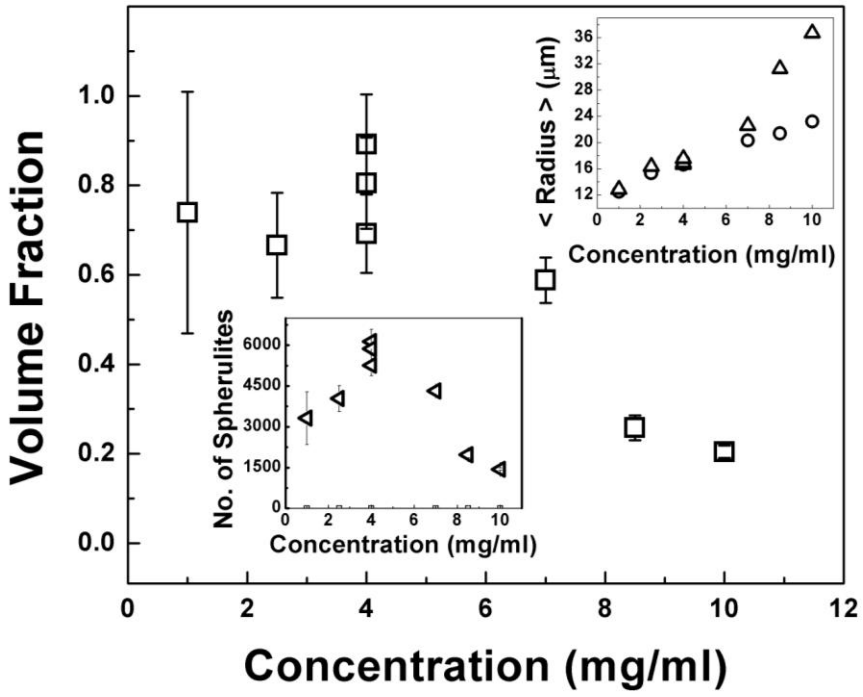

FIGURE 7 The balance between spherulites and fibrils as a function of BPI concentration. Main panel: volume fraction (see equation 2 in the main text) of protein in spherulites (T= 60˚C, 25mM NaCl, pH 1.75) (□).Bottom left inset: number of spherulites as a function of BPI concentration. Top right inset: spherulite radii as a function of BPI concentration (○). The upwards triangles in the top right inset show the radius of the spherulites predicted from equation 4.